ISSN: 0975-833X

Available online at http://www.journalcra.com

International Journal of Current Research
Vol. 15, Issue, 06, pp.25088-25099, June, 2023
DOI: https://doi.org/10.24941/ijcr.45540.06.2023

INTERNATIONAL JOURNAL OF CURRENT RESEARCH

RESEARCH ARTICLE

ASSESSMENT OF FORAGE PRODUCTION IN PASTORAL RANGELANDS USING MULTISPECTRAL DRONE IMAGERY DATA IN THE SAHELIAN AND SUDANIAN ZONES OF THE WEST AFRICAN SAHEL

***,[1,2] Issaka BOUBACAR ALI, [2]Issa GARBA, [2]ZAKARI SEYBOU Abdourahamane, [3]Illa SALIFOU and [4]Maxime BANOIN**

[1]Abdou Moumouni University (UAM), Department Animal Production, Agronomy Faculty, Niamey BP: 10960, Niger; [2]Regional Centre AGRHYMET (CRA), Information and Research Department (DIR), Niamey BP: 11011, Niger; [3]Institut des Radio-Isotopes (IRI), Niamey BP : 1727, Niger ; [4]Laboratory of Improvement of Animal Productions in Arid and semiarid Zones (LAPAZAS), Abdou Moumouni University (UAM), Niamey BP: 10960, Niger

ARTICLE INFO

Article History:
Received 24th March, 2023
Received in revised form
14th April, 2023
Accepted 20th May, 2023
Published online 30th June, 2023

Key words:

Drone, multispectral, biomass, herbaceous, ligneous, RLS

**Corresponding Author:*
Issaka BOUBACAR ALI

ABSTRACT

The forage mass of herbaceous and woody plants is the main source of food for livestock in pastoral rangelands in the Sahelian and Sub-Danian zones. This study aims to assess the biomass of woody and herbaceous species using the normalized difference vegetation index NDVI derived from multispectral Red-Green-Blue and near-infrared drone images and photogrammetric parameters. A DJI Phantom multispectral UAV was used to collect images from four pilot sites in Niger and Benin. Ground measurements of herbaceous biomass using the integrated yield square method and estimation of woody leaf phytomass using dendrometric parameters calculated with allometric equations were used to assess the performance of the drone-based model. The results showed that the herbaceous biomass estimated with the drone had an R^2 coefficient of determination of 0.59-0.86 and relative root mean square estimation errors (RMSEr) of 19.86% to 26.84% with ground measurements, at a significance level of $p < 0.0001$. As for woody biomass, an R^2 of 0.58-0.69 and an RMSEr of 14.16% to 39.55% at a p-value < 0.0001 were obtained.

Citation: ***Issaka BOUBACAR ALI, Issa GARBA, ZAKARI SEYBOU Abdourahamane, Illa SALIFOU and Maxime BANOIN.*** **2023.** Assessment of forage production in pastoral rangelands using multispectral drone imagery data in the sahelian and sudanian zones of the west african sahel*". International Journal of Current Research*, 15, (06), 25088-25099.

INTRODUCTION

Livestock plays an important role in the national economies of Sahelian countries, contributing 40% of agricultural Gross Domestic Product (GDP) and 44% of agricultural GDP in West African countries (CEDEAO, 2008). In Niger, livestock farming is practiced by over 87% of the population, making it the country's second most important economic activity after agriculture. It accounts for almost 11% of national added value and 40% of agricultural GDP (CILSS /RPCA, 2010). In Benin, this sector is also the country's second-largest agricultural activity, accounting for 2.4% of GDP (FAO,2015). Despite its importance in the economy, the livestock farming system remains traditional in these two countries. It is practiced in a traditional way and is essentially based on the exploitation of natural fodder subject to strong inter- and intra-seasonal variability (Garba *et al.,* 2015).

In both countries, natural pastures are essentially made up of annual forage biomass (herbaceous and woody), which is also the main source of animal feed (Hiernaux *et al.,* 2015).Data collection on forage biomass in this region is generally carried out by destructive sampling in the field, a costly, time-consuming and energy-intensive method, particularly in the semi-arid zones of the Sahel where productivity per unit area is low and highly variable from one year to the next. In recent decades, the use of spatial remote sensing has become an important approach to estimating biomass (Barrachina *et al.,* 2015; Diouf *et al.,* 2015; Garba *et al.,* 2015; Reinermann *et al.,* 2020). Vegetation indices derived from satellite data are widely used to monitor biomass productivity(Diouf *et al.,* 2015; Gao *et al.,* 2013). By combining these indices with field measurements, it is possible to assess the quantity of biomass produced and provide decision-makers with useful information for natural resource management. This approach also reduces or eliminates the need for time-consuming field measurements, while characterizing vegetation and mapping pastoral resources (Bossoukpe, 2021; Taugourdeau *et al.,* 2022). The accuracy of biomass estimates depends on the

resolution of the images used. To obtain an accurate estimate, it is often recommended to use higher spatial resolutions than those generally provided by satellite images (Read *et al.,* 2003). However, images from very high-resolution commercial satellites, such as Deimos-2, GeoEye-2, Quick Bird or WorldView-2, are expensive and can be affected by cloud cover depending on the period. In some cases, the high cost may make the use of these images uneconomical, particularly if several images from different dates are required, or if large areas need to be covered. Drones are an interesting solution in these contexts, as they are more affordable, flexible, can fly below the clouds and produce very high-resolution images with centimeters-level accuracy (Ndamiyehe *et al.,* 2020).

Processing these images using photogrammetric techniques such as "Structure from Motion" generates ortho-images and Digital Surface Models (DSMs), which allow us to estimate the height, volume and surface of objects (Cunliffe *et al.,* 2016;Anifantis *et al.,* 2019; Sarron, 2019; Bourgoin *et al.,* 2020;).Vegetation indices derived from ortho mosaics can be calculated using RGB sensors(Lussem *et al.,* 2019; Taugourdeau *et al.,* 2022) or multispectral captures (Surault *et al.,* 2018). These vegetation indices, combined with biophysical data in the field, allow us to estimate the phytomass (herbaceous and woody) (Bossoukpe *et al.,*2021; Peciña *et al.,* 2021)or crop biomass (Roupsard *et al.,* 2020). Despite this, there are few studies on the use of drones to study natural vegetation in Sudanian and Sahelian zones. Most scientific studies of natural vegetation in Africa have been carried out in humid tropical regions (Ngabinzeke*et al.,* 2016). In addition, studies using the "Structure from Motion" (SFM) process have mainly been carried out in temperate grasslands and on a local scale(Lussem *et al.,*2019; Wijesingha *et al.,* 2020). The aim of the present study was to evaluate the performance of a drone system equipped with multispectral sensorsin estimating forage biomass in pastoral rangelands of the Sahelian and Sudanian zones of West Africa, in order to develop a decision-making tool.

MATERIALS AND METHODS

Study Area: The study was conducted in two countries: Niger, in the Dosso region, and Benin, in the Alibori department. In the Niger region, the communes of Falmey and Dioundiou were grouped together to form the study area, located between latitudes 12°0'0" and 13°0'0" North, and longitudes 2°0'0" and 4°0'0" East (Figure 1). The climate of this region is Sahelo-Sudanian, characterized by two distinct seasons: a long dry season lasting eight to nine months, generally from October to May, and a short rainy season from June to September (DRE,2022). The region's vegetation comprises a number of formations, including arbustive savannahs on the plateau, parks with *Vitellaria paradoxa* and *Parkia biglobosa*, and the Dallols Bosso and Maouri *rôneraie*, whose key species is *Borassus aethiopum* (Mahamane, 2004).

In Benin, the study was carried out in the communes of Malanville and Gogounou, located in the north-western Alibori department, between latitudes 11°0'0" and 12°0'0" North, and longitudes 2°0'0" and 4°0'0" East (Figure 1). The region's climate is tropical Sudanian, with two distinct seasons: a dry season from October to April, and a rainy season from May to September. Average annual rainfall ranges from 677 mm in the north to 1060 mm in the south. Average monthly temperatures range from 25°C in the south to 33°C in the north (Météo Bénin, 2018).The region's vegetation consists mainly of savannah dotted with patches of open forest, crossed by gallery forests. These savannah-cultural formations are frequently exposed to the risk of bush fires during the dry season (Hountondji, 2008).

Overall methodology: To carry out this study, we have set up a sampling protocol that combines various techniques, including photogrammetry, stereoscopy and the use of ground data. The aim of this protocol is to analyze biomass using very high spatial resolution images acquired using a drone (Figure 2).

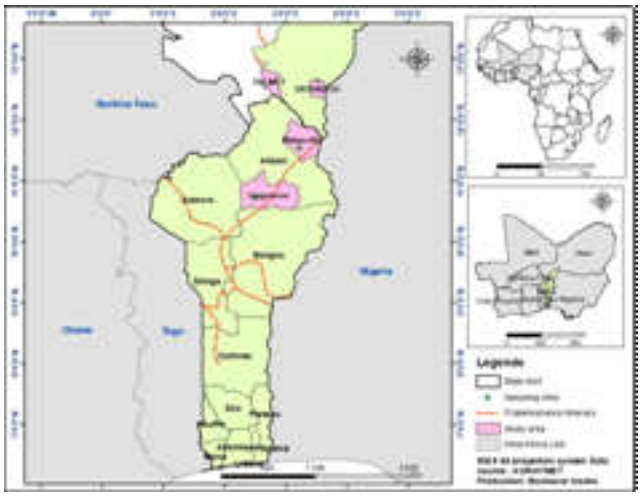

Figure 1. Geographical location of the study area

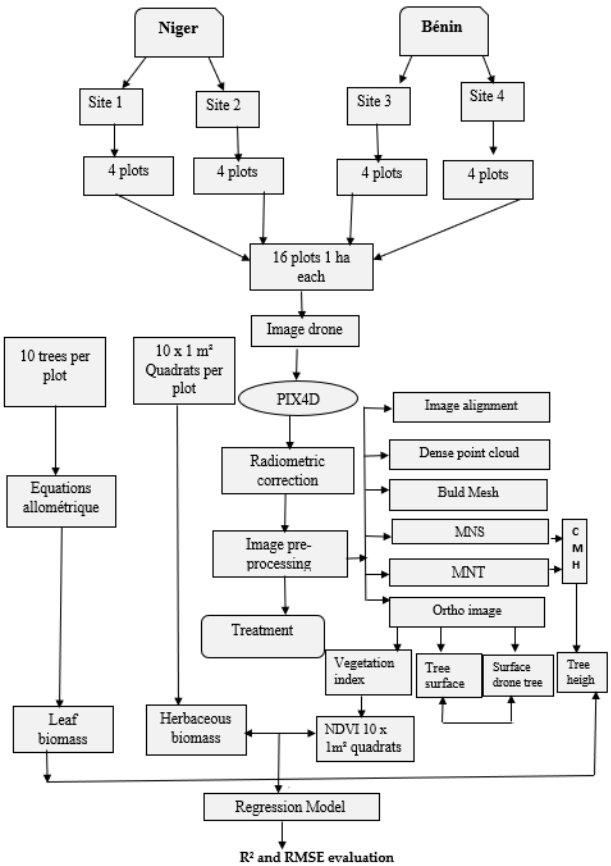

Figure 2. Overall methodology of study

Sampling sites: This study was carried out on four pastoral test sites located in the Dosso region of Niger and in the Alibori department of Benin. The sites are located in the communes of Falmey and Dioundiou in the Dosso region, and in the communes of Malanville and Gogounou in the Alibori department (see Figure 1). The choice of these sites was based on several criteria, including the north-south gradient along the cross-border transhumance corridor (Dosso - Nord - Benin), the availability of in situ data, the bioclimatic gradient and environmental accessibility. The characteristics of the sampling sites are presented in Table 1.

Collecting device : The data collection system was set up at the four pastoral sites. On each site, a total of 16 one-hectare plots were delimited, or four plots per site in Niger and Benin. Two types of measurement were carried out: drone over flight measurements and ground measurements, including herbaceous and woody species.

Table 1. Characteristics of sampling sites

N	Site name	Agroecological zone	Communes	Country
1	Kara	Sahelo- Sudanese	Falmey	Niger
2	Tombo mochè	Sudanese	Dioundiou	Niger
3	Golabanda	Sudanese	Malanville	Bénin
4	Oroubeidou	Sudanese	Gogounou	Bénin

General presentation of the measure system: The measurement system used in this study is a DJI (Da Jiang Innovation) drone, specifically the Phantom 4 multispectral model, which offers extremely high resolution and multispectral imaging capabilities (Figure 3). It is a four-motor quadcopter drone powered by a 5870 mAh LiPo (lithium polymer) smart battery, operating at 12.5 volts and offering 28 minutes of autonomy. With a wingspan of 20 cm, a weight of 1487 g, a maximum speed of 54 km/h and a maximum flight altitude of 500 m, this drone is capable of exceptional performance. The Phantom 4's multispectral imaging system comprises six cameras with 1/2.9-inch CMOS sensors, including an RGB camera and a multispectral camera array. This array comprises five cameras covering the blue (450 nm), green (560 nm), red (650 nm), red edge (730 nm) and near infrared (840 nm) bands. Each camera has a resolution of 2 MP (megapixels) and is mounted on a three-axis stabilized nacelle (Figure 4). To guarantee accuracy and image quality, all the cameras in the system undergo a calibration process. This process enables radial and tangential lens distortions to be measured and recorded in the metadata of each image, facilitating subsequent pre-processing. Images are acquired automatically, at a rate previously defined during flight preparation. What's more, the drone is equipped with an on-board D-RTK antenna that provides positioning data accurate to the nearest centimeter. Safety is also taken into account with multidirectional obstacle detection activated by front, rear, bottom and infrared optical sensors. An integrated spectral sensor, positioned above the drone, captures solar irradiance to maximize the accuracy and consistency of data collection at different times of the day. The system also uses autonomous flight technology based on ultrasonic sensors to reduce the risk of accidents. In addition, it is equipped with a GPS-BeiDOU-Galileo; GPS-GLONASS-Galileo location system to ensure precise localization. Communication between the drone and the ground station is via a radio control system operating in the 2.400 to 2.4835 GHz frequency range. Under normal conditions, with no obstacles hindering radio signal transmission, this communication can extend over a maximum distance of 10 km. This enables real-time visualization of image and video sequences on the control station. Thanks to its digital technology, the radio control unit has an autonomy of 1.5 hours.

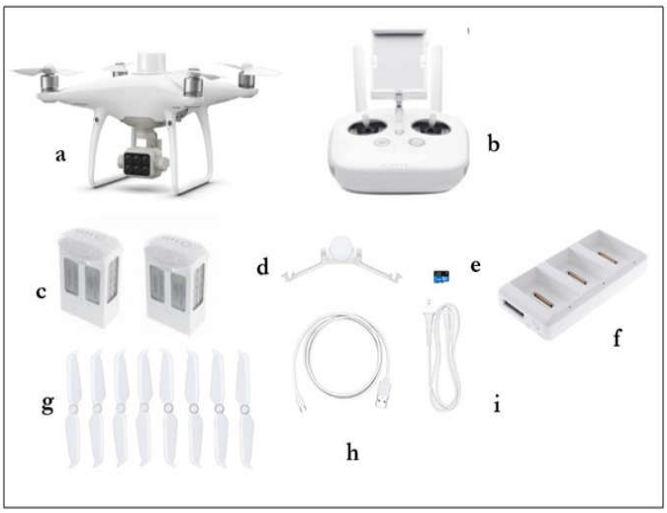

Figure 3. Drone DJI Phantom 4 multispectral and accessories (a) DJI Phantom 4 multispectral b) Radio control. c) Battery. d) Nacelle. e) USB card. f) Charging platform. g) Propellers. h) Cable iPad. i) Charger cable

Planning and acquisition of aerial images by drone: The planning and acquisition of aerial images by drone was carried out methodically and precisely.

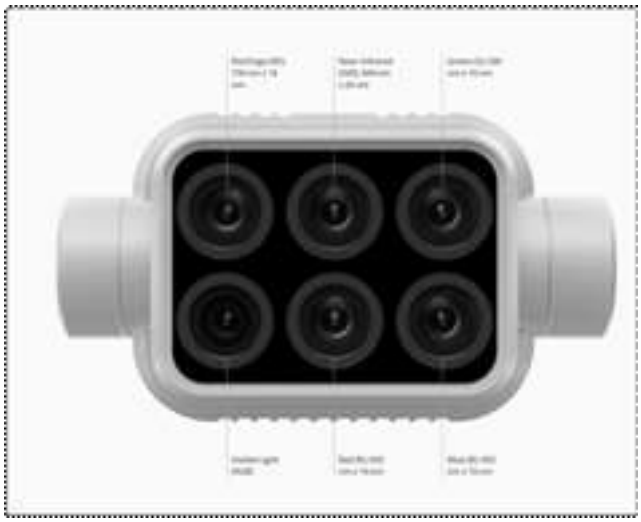

Figure 4. Presentation of the UAV sensor

We used the Gspro (Ground Station Pro) application to configure the drone and plan the flight in automatic mode. Aerial images were captured at a flight altitude of 90 m for each of the four pastoral sites, with a ground resolution of 4.9 cm/pixel. Each image covers a footprint of 1600 x 1300 m and is captured in the visible light spectrum (Red, Green and Blue) as well as the near infrared. Flights took place between 9am and 12pm to minimize shadowing effects on the images. In addition, flights were timed to coincide with ground data collection at each site, thus ensuring optimum synchronization. The average horizontal flight speed was maintained at 5 m/s to ensure accurate image acquisition, thus avoiding SD card recording problems that could occur at high speeds. Frontal overlap of around 70% and lateral overlap of around 75% were applied between photos taken on the same line and row, respectively. These levels of overlap enable images to be properly stitched together during photogrammetric processing, ensuring high-quality results (Ngabinzeke*et al.,* 2016; Khun, 2021). Flight planning was carried out using a grid and polygonal plan, defining the lines and rows the drone was to follow during the flight. A total of four flight plans were drawn up, each comprising five parallel flight lines or transects in a north-south direction. This enabled us to fly over the four-pastoral par-courses, each covering an area of one hectare, ensuring complete coverage of the study area (Figure 5).

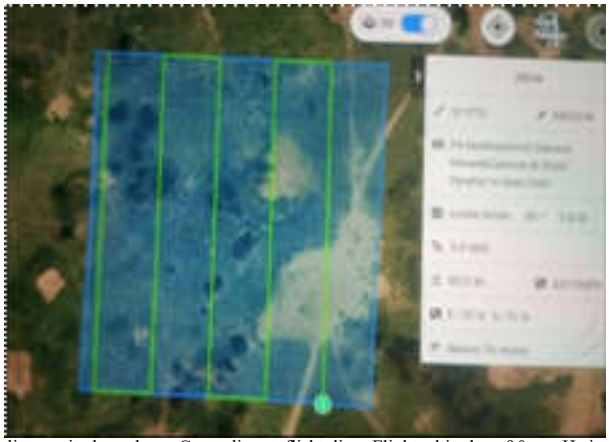

Blue line = site boundary; Green line = flight line; Flight altitude = 90 m; Horizontal flight speed = 5 M/S; Longitudinal overlap = 70% and lateral overlap = 75% Image resolution = 4.8 CM/PX

Figure 5. Flight plan for site 1

Field measurements: Herbaceous biomass data were collected in October 2022, corresponding to the vegetative growth period of Sahelian and Sudanian rangelands. Once the flyover was completed, we randomly selected ten one-square-meter (1m²) quadrats from each of the 16 one-hectare plots.

GPS coordinates were collected from the center of each quadrant. Biomass was estimated using the integral harvesting method for yield squares (Daget & Poissonet, 1971)for each sampling point. This method consists of cutting all herbaceous species present in the 1m² quadrant at ground level, including grasses, legumes and others. All individuals within the quadrant were harvested. The fresh biomass obtained was weighed using a load cell. After being dried in an oven, the biomass was weighed again to obtain the dry weight. The biomass was then transported to the Carbon Laboratory of the Centre Regional AGRHYMET (CRA), where it was oven-dried for three days at 70°C (Figure 6).

Figure 6. Biomass oven drying at 70°C

Tree measurements were carried out in January 2023 on 16 plots distributed over the four sites in the study area. On each of the 16 plots, we selected 10 mature trees (> 1.3 m in height; > 5 cm in trunk diameter) to cover the diversity of tree morphology present. This selection enabled us to obtain small, medium and large-sized woody individuals. Den-drometric measurements were taken on single-trunk trees at ground level and on shrubs at 30 cm above ground level. We recorded the following parameters: stem diameter, total height (Ht) and North-South (NS) and East-West (EO) crown diameters.

Calculation of crown area: Crown area was calculated using the following formula to first obtain the average horizontal projection radius (R) from the average crown diameters: R = (DH (NS) + DH (EO)) / 4, where R represents the average radius, DH (NS) is the crown diameter in the North-South direction, and DH (EO) is the crown diameter in the East-West direction. The crown area (SH) was then calculated for each tree using the universal formula for the area of a cylinder: $SH = \pi R^2$.

Determination of tree height (CMH) using photogrammetry: Ortho-photos obtained from drone flights were processed with PIXI4D software to obtain Digital Surface Models (DSMs) and Digital Terrain Models (DTMs). Tree heights were determined by calculating the difference between DSMs and DTMs using ArcGIS software and the following formula: CHM = MNS – MNT, where CHM represents the canopy height model, MNS is the Digital Surface Model (where the pixel value represents the object's altitude and height) and MNT is the Digital Terrain Model.

Aerial image analysis: Multispectral images taken by the Phantom 4 were processed using the photogrammetry software PIX4D mapper 4.5.6. PIX4D is a robust commercial software package specifically designed for processing images from UAVs. It is based on Structure from Motion algorithms and also incorporates computer vision techniques and photogrammetric algorithms (Puliti *et al.,* 2015; Lussem *et al.,*2019; Panday *et al.,* 2020;; Wijesingha *et al.,* 2020)**,** in order to achieve high accuracy in aerial image processing(Ruzgienė *et al.,* 2015; Zahawi *et al.,*2015). PIX4D calculates the key points of individual images and uses them to find matches between different images.

From these initial matches, the software iteratively performs a number of steps, including automatic aerial triangulation, packet block adjustment and camera auto-calibration, until an optimal reconstruction is achieved (Fernández-Guisuraga *et al.,* 2018; Panday *et al.,* 2020). Next, a densified point cloud is generated to create a highly detailed Digital Surface Model (DSM) and Digital Terrain Model (DTM), which will be used to generate the final orthomosaics and reflectance maps for each site (Figure 7). The reflectance maps were generated by applying radiometric calibrations and corrections. Firstly, a radiometric calibration was carried out using calibration target images that provide an absolute reference of radiometry, enabling data from several flights to be compared. Next, "Camera and Sun irradiance" radiometric corrections were applied to correct for terrain reflectance. In this process, Pix4D mapper uses the ISO values, aperture, shutter speed, sensor response, optical system and vignetting recorded in the textual metadata files (EXIF and XMP tags) for each photogram, to correct the camera parameters. Next, incoming sunlight irradiance is corrected based on in-formation provided by the solar irradiance sensor. This sensor provides data on light conditions during the flight, in the same spectral bands as those captured by the multispectral sensor, and this information is recorded in the textual metadata files mentioned above. This "Camera and Sun irradiance" correction normalizes the images captured during the flight, enabling comparison of images taken under different illumination conditions. Pix4D mapper applies this calibration and correction process to each photo-gram just before generating the final reflectance orthomosaics for each spectral band (Figure 7).

Site-specific vegetation index extraction and forage biomass prediction methods: We used Pix4D software to calculate the normalized difference vegetation index (NDVI) using spectral reflectance values in the red, green and near-infrared bands. This enabled us to assess phytomass. NDVI is a commonly used index for estimating the presence of vegetation in an area(Taule *et al.,* 2012 ; Candiago *et al.,* 2015; Garba *et al.,* 2015). It is calculated by taking the ratio between the difference in reflectance in the near-infrared band and the reflectance in the red band. The index varies from -1 to 1, where -1 indicates a total absence of vegetation and 1 indicates an absolute presence of vegetation (Figure 8). In our study, NDVI was used to predict herbaceous biomass. It is calculated using the following formula:

$$NDVI = \frac{(PIR - R)}{(PIR + R)}$$

The prediction of herbaceous phytomass in different pastoral sites was carried out using the dry herbaceous biomass of the quadrats and the vegetation index values (Figure 9). The geographical coordinates of the biomass measured on the ground of each quadrat of the different one-hectare plots were superimposed on the calculated vegetation index maps. Buffer zones were defined around each GPS point to simulate the quadrat using ArcGIS software. A mask was applied to each quadrat to extract the mean values of the pixels corresponding to each 1m² quadrat, using Envi 5.3 software. The average vegetation index value of the pixels contained within this buffer zone was used to define the quadrats vegetation index value. These values were entered into an attribute table in the Excel file and used for statistical analysis. Woody phytomass was determined for the entire study area using a linear regression model linking field measurements (dendrometric parameters) and photogrammetric measurements (tree height, crown area). On each one-hectare drone orthomosaic, we first delimited the leaf area often manually selected trees using ArcGIS software (Figure 10-a). We then used allometric equations to calculate the above-ground biomass of the ten woody individuals in each one-hectare plot.These species include *Balanites aegyptiaca* (Adamou *et al.,* 2020), *Guiera senegalensis* (Henry *et al.,* 2011),*Combretum micranthum*(Sawadogo *et al.,* 2010)**,** *Combretum nigricans*(Sawadogo *etal.,* 2010),*Combretum glutinosum*(Mbow *et al.,* 2014), *Detarium microcarpum*(Koala, 2016), et *Vitellaria paradoxa* (Koala, 2016). For species for which no allometric equations are available (*Cassia sieberiana, Lannea acida*, *Combretum collinum*), we used the pantropical equations (Brown, 1997).

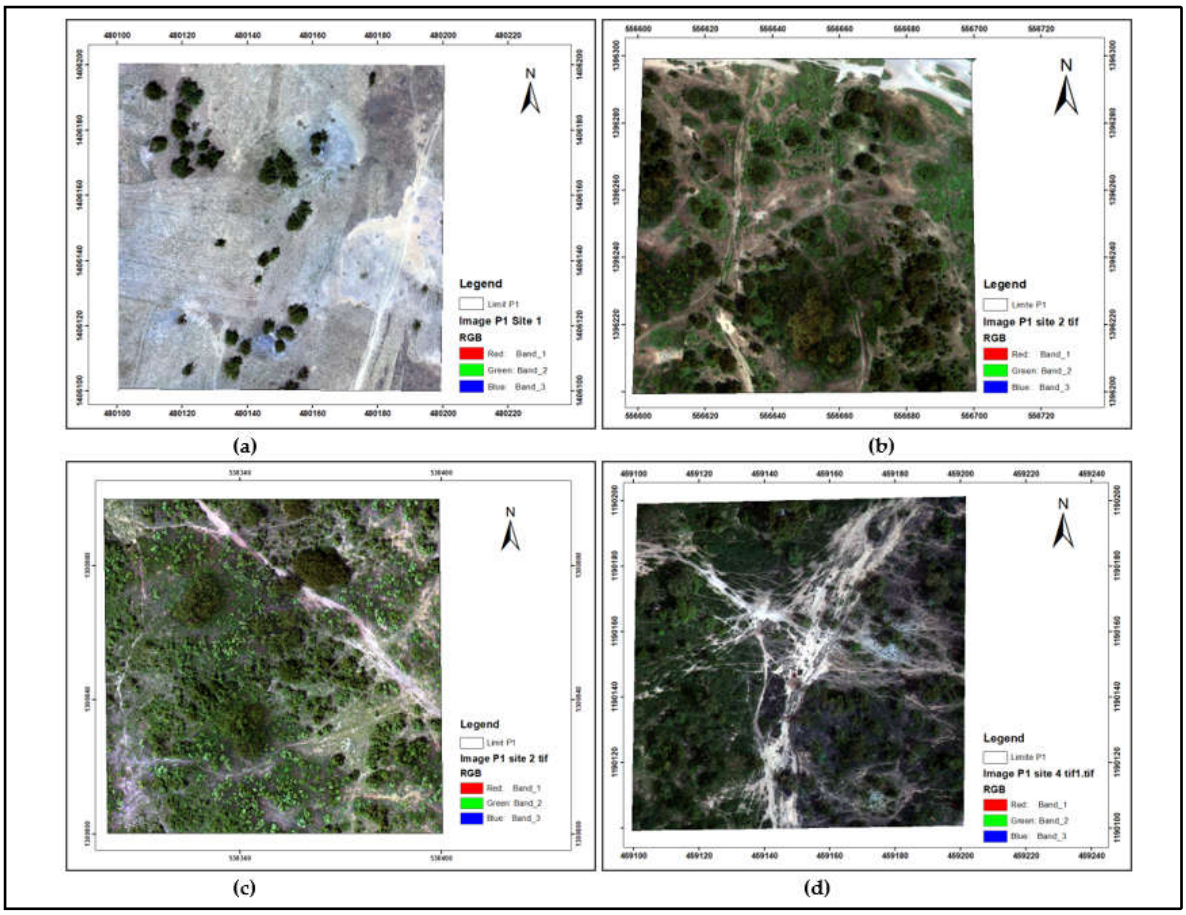

Figure 7. Orthomosaic examples of one-hectare pastoral plots in color composition: NIR (near infrared) + Red + Green; (pixel resolution: 4.9 cm) for each site (a = site 1; b = site; site 3 = c; site 4 = d)

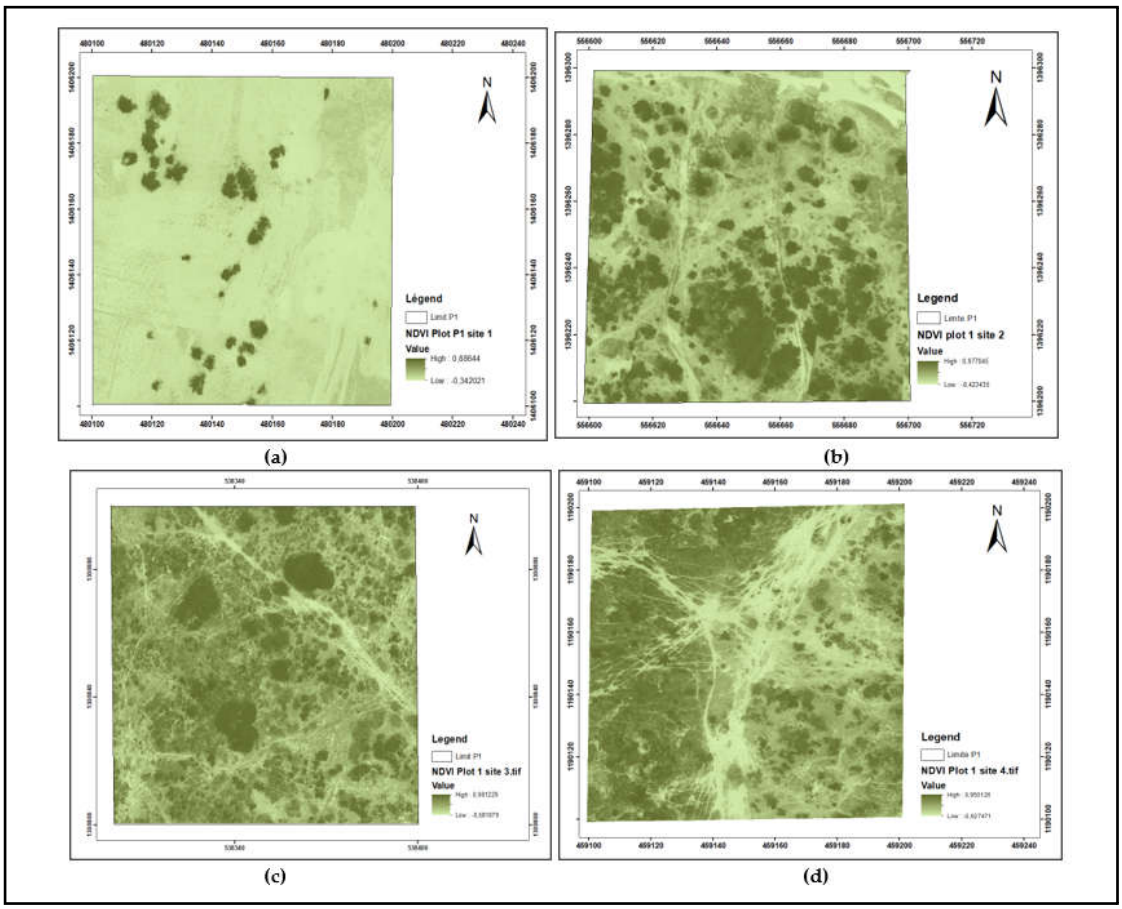

Figure 8. Drone NDVI vegetation index of one-hectare pastoral plots at each site (a = site 1; b = site 2; site 3 = c; site 4 = d)

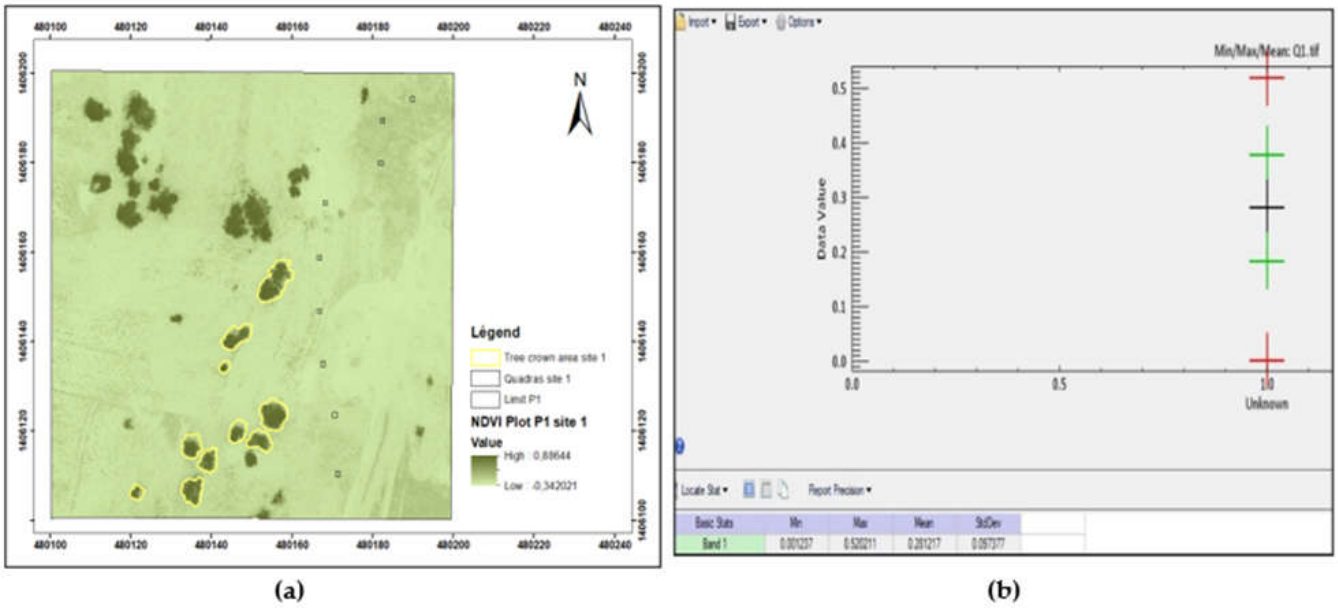

Figure 9: (a) Drone NDVI vegetation index map and masking (a); Calculation of the mean value of a quadra (b)

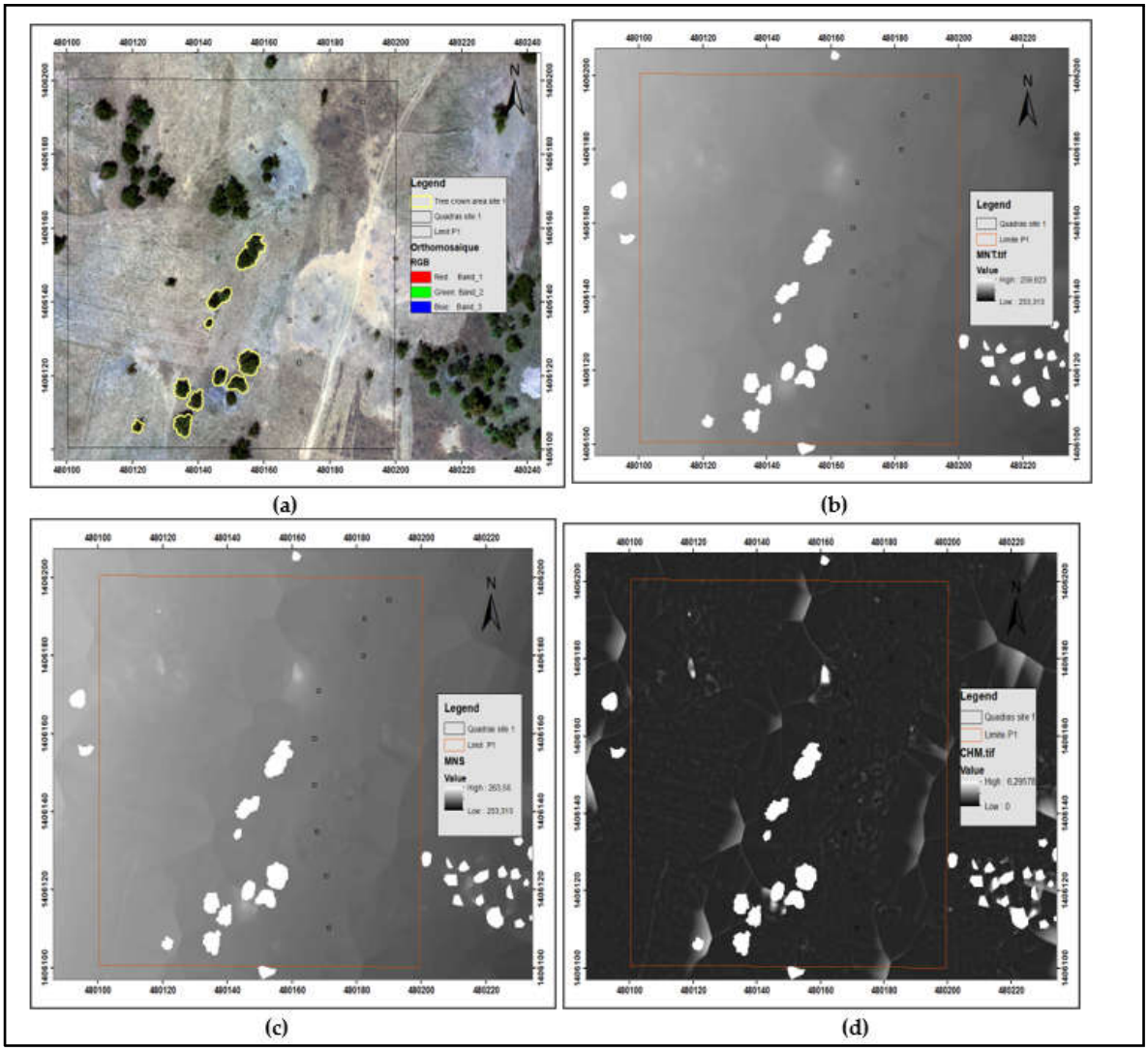

Figure 10. Orthomosaic of a one-hectare plot at site 1 (a); Digital Terrain Model (DTM) (b); Digital Surface Model (DSM) and (a) Canopy Height Model (CHM)

From the raster outputs (DSM, DTM), total tree height was calculated by subtracting the Digital Surface Model (DSM) from the Digital Terrain Model (DTM) using ArcGIS software (Figure 10). Finally, relationships were established between these measurements extracted from UAV images and direct measurements obtained in the field, in order to predict woody phytomasse across the entire study area.

Statistical data analysis: In this study, Simple Linear Regression (SLR) was used to predict woody and herbaceous phytomass using R software and the least-squares method. For the prediction of herbaceous phytomass, regression models were established by relating the herbaceous biomass measured in the ground quadrats to the mean of the NDVI vegetation index values corresponding to each quadrat. For woody phytomass, relationships were established between the fo-liar biomass calculated from allometric equations and that obtained using dendrometric parameters of trees extracted from UAV images.

The performance of each phytomass estimation model was evaluated using the R^2 coefficient of determination. This coefficient gives a general indication of model fit. To assess model accuracy, we also used the root mean square error (RMSE) and the relative root mean square error (RMSEr). These measures enable us to determine which model provides the best results. The Akaike Information Criterion (AIC) was used to compare the performance of different models. The AIC has recently been used to compare models in other studies that have estimated biomass based on remotely sensed data (Gleason & Im, 2012; Pham *et al.,* 2017).

$$RMSE = \sqrt{\frac{\sum_{i=1}^{n}(Xobs,i - Xest,i)^2}{n}}$$

Where xobs,i; xest,i, i and n represent observed biomass, estimated biomass and number of samples, respectively.

RESULTS

Analysis of herbaceous biomass

Relationship between grass biomass measurements of ground quadrat and the NDVI vegetation index corresponding to each quadrat on the pilot sites: We used simple linear regression to assess the relationship between quadrat biomass and NDVI (Figures 11). Analysis of these results reveals that each model has a coefficient of determination R^2 close to 1, indicating a strong and significant correlation between quadrat biomass and NDVI. The points in the data cloud are very close to the regression curve. Statistical precision (Table 2) confirms the significance of the relationships, with a p-value<0.0001. The coefficients of determination R^2 are 0.61, 0.86, 0.79 and 0.59 respectively for sites 1, 2, 3 and 4. Furthermore, these results show that the highest coefficient is observed in the Sudanian zone (site2).

Woody biomass analysis

Relationship between photogrammetric measurements (leaf area, height) and field measurements of total height and crown area of trees: On all four study sites, we observed significant correlations

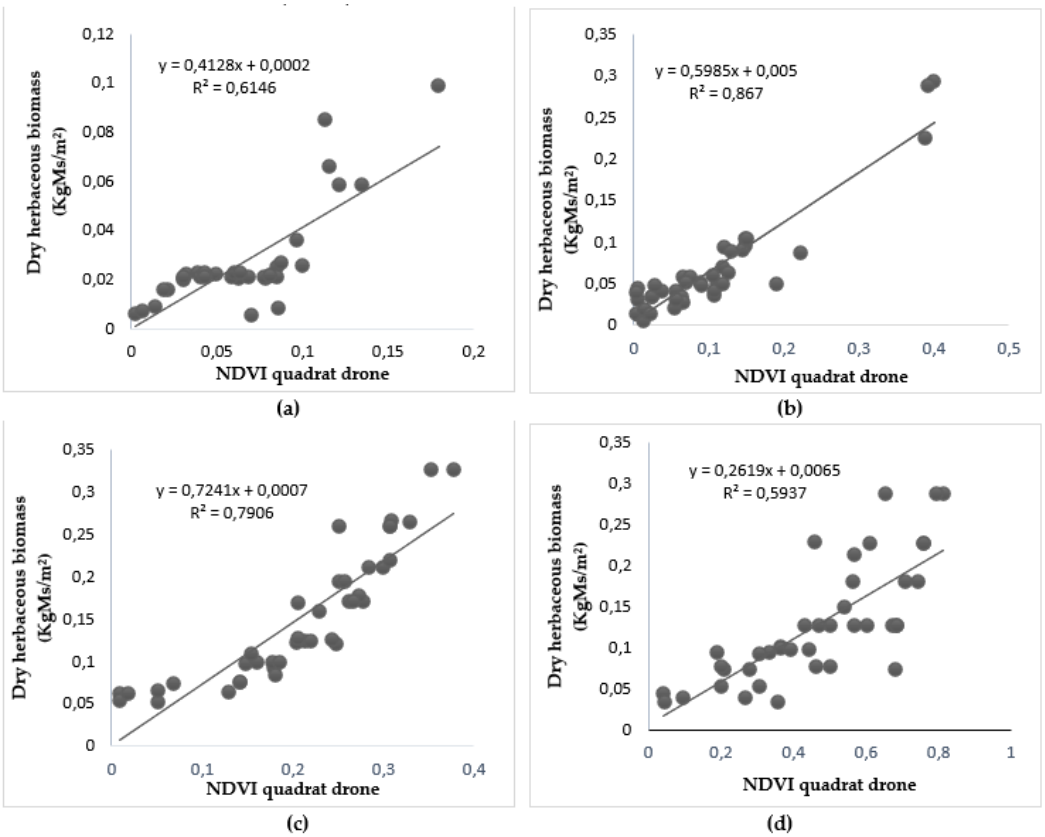

Figure 11. Relationship between measured herbaceous biomass of site ground quadrats and quadrat NDVI (a = site 1; b = site; site 3 = c; site 4 = d)

Table 2. Statistical models for estimating herbaceous phytomass and their accuracies

Study sites	Equation	R^2	R^{*2}	RMSE KgMs/m²	RMSEr %	AIC	P-value
Site 1	y = 0,5985x + 0,005	0,61	0,60	0,014	22,82	182,51	$2{,}1910^{-9}$
Site 2	y = 0,4128x + 0,0002	0,86	0,86	0,110	26,11	181,66	$2{,}210^{-16}$
Site 3	y = 0,7241x + 0,0007	0,79	0,78	0,035	19,86	148,57	$1{,}810^{-14}$
Site 4	y = 0,2619x + 0,0065	0,59	0,58	0,046	26,84	127,03	$6{,}0610^{-9}$

y: Biomass herbaceous; x: NDVI, R^2: coefficient of determination, R^{*2}: adjusted coefficient of determination, AIC: Information criteria of Akaike, RMSE: root mean square error estimation, RMSEr: relative root means square estimation errors

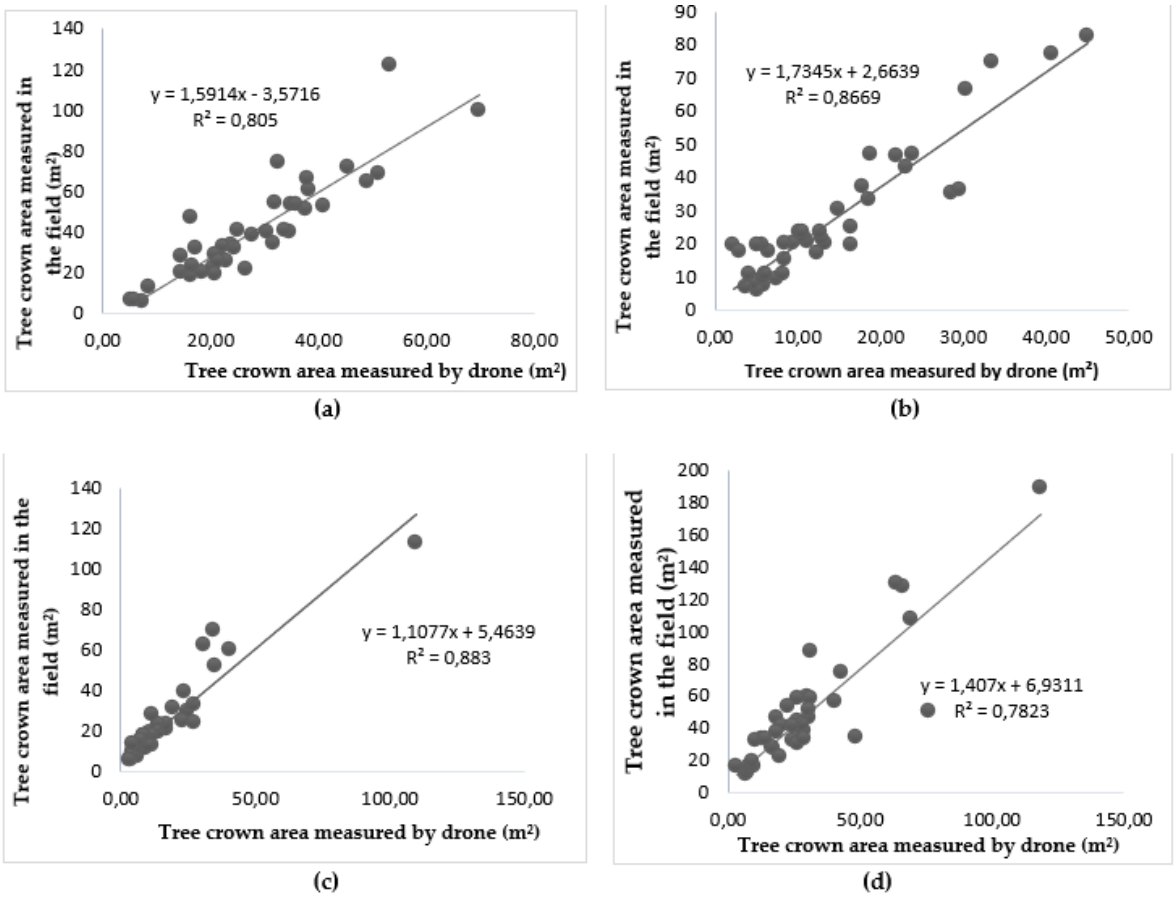

Figure 12. Relationship between crown area measured by drone and that measured on the ground (a = site 1; b = site; site 3 = c; site 4 = d)

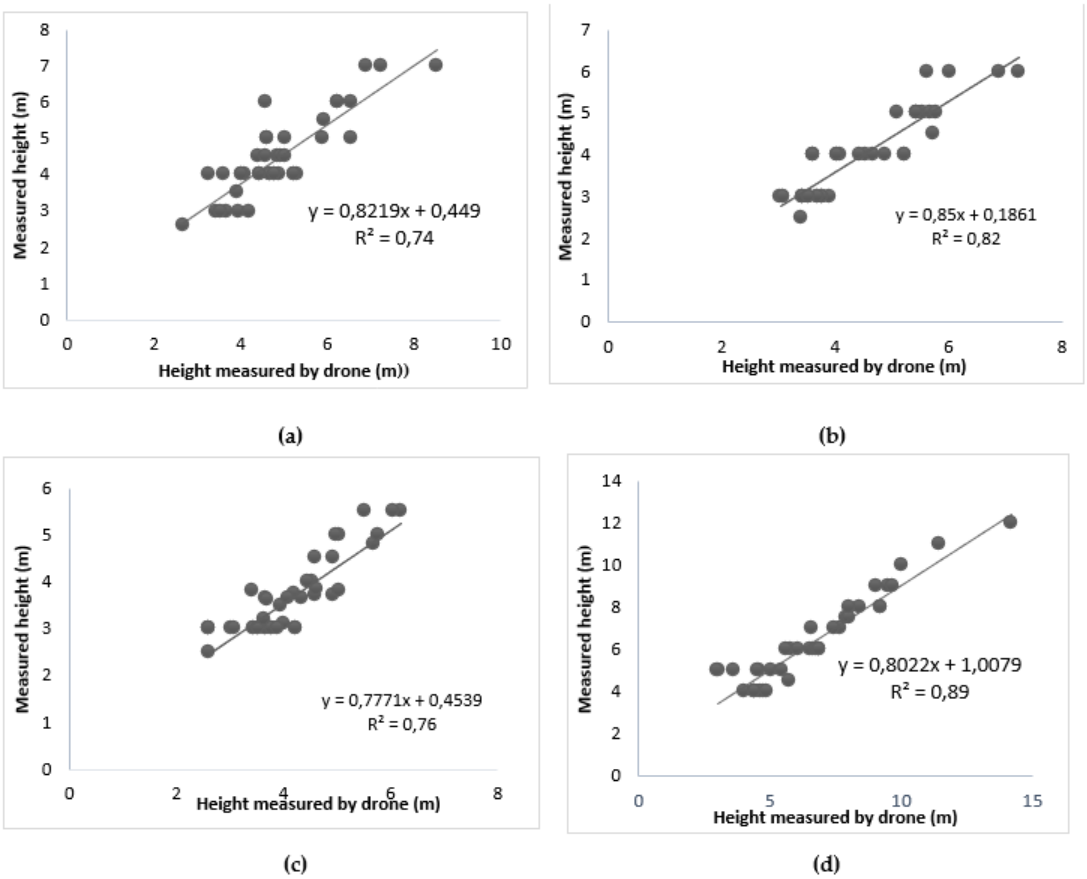

Figure 13. Relationship between height measured by drone and height measured on the ground (a = site 1; b = site; site 3 = c; site 4 = d)

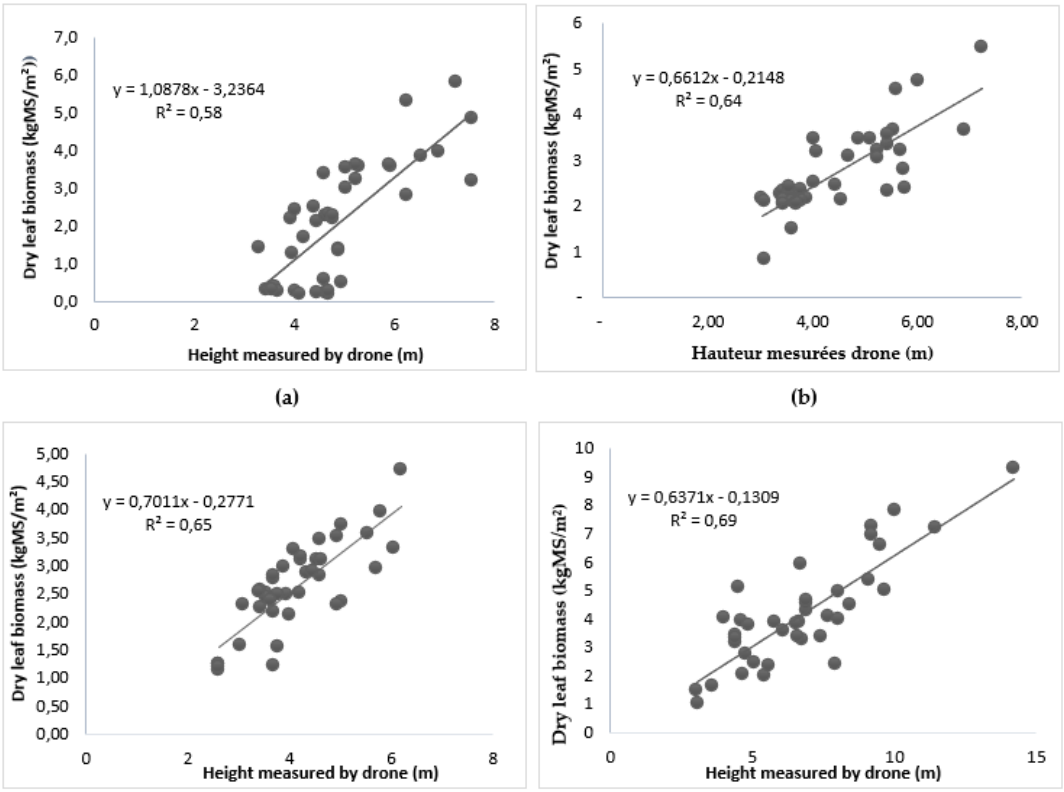

Figure 14. Relationship between leaf biomass and total tree height from photogrammetric measurements (a = site 1; b = site; site 3 = c; site 4 = d)

Table 3. Statistical models for estimating woody phytomass and total tree height from photogrammetric measurements and their accuracies

Study sites	Equation	R^2	R^2*	RMSE KgMs/m²	RMSEr %	AIC	P-value
Site 1	y = 1,0878x - 3,2364	0,58	0,57	0,99	39,55	119,19	$8{,}77\ 10^{-9}$
Site 2	y = 0,6612x - 0,2148	0,64	0,63	0,53	14,16	68,81	$4{,}9610^{-10}$
Site 3	y = 0,7011x - 0,2771	0,65	0,64	0,56	14,72	58,51	$1{,}4710^{-11}$
Site 4	y = 0,6371x - 0,1309	0,69	0,68	0,98	19,28	116,62	$3{,}9610^{-11}$

y: Leaf biomass x: tree height, R^2: coefficient of determination, R^2*: adjusted coefficient of determination, AIC: Information criteria of Akaike, RMSE: root mean square error estimation, RMSEr: relative root means square estimation errors

between variables measured in the field (crown area and total tree height) and those determined from the drone. Comparison of the crown area measurements assessed in the field with those obtained from the drone revealed a strong correlation, with coefficients of determination (R^2) between 0.78 and 0.88 and a p-value < 0.0001 (Figure 12). Similarly, the comparison of crown area measurements evaluated in the field with those determined by drone shows a significant correlation, with R^2 values ranging from 0.74 to 0.89 and a p-value < 0.0001. The strongest correlation is observed at site 4 (Figure 13).

Relationship between leaf biomass and total tree height from photogrammetric measurements: Analysis of Figure 14 highlights the relationship between leaf biomass and total tree height obtained from drone images. The trend line for biomass as a function of height reveals R^2 coefficients varying between 0.58 and 0.69. These R^2 values demonstrate a very strong correlation between leaf biomass and total height measured by photogrammetry. Statistical precision (Table 3) indicates that these relationships are significant for all sites.

DISCUSSION

Estimating herbaceous and woody biomass is an essential step in assessing arid and semi-arid ecosystems (Bossoukpe *et al.,* 2021; Nungi-Pambu, 2022; Taugourdeau *et al.,* 2022).

In this study, we demonstrated that the use of low-cost multispectral UAVs enables efficient estimation of herbaceous and woody biomass. The production of the biomass map is based on a linear regression equation between the mean value of the NDVI (Normalized Difference Vegetation Index) of each 1m² quadrat and parameters derived from dendrometric measurements. Drone outputs explain between 61% and 86% of the variance for herbaceous biomass and between 58% and 69% for woody biomass. The NDVI vegetation index is strongly related to herbaceous biomass. Mean prediction errors (RMSE) ranged from 0.013 kgMs/m² to 0.110 kgMs/m², with relative errors of 19.86% to 26.84% for dry mass. The greatest error was observed at site 4 in the Sudanian zone. Numerous studies have confirmed the use of drones for biomass assessment (Surový *et al.,* 2018; Taugourdeau *et al.,* 2022; Wijesingha *et al.,* 2020).

Our results are consistent with the literature, where other authors have obtained similar regression coefficients between vegetation index and biomass measured on the ground (Carlos A. *et al.,*2019; Liu *et al.,* 2019; Taule *et al.,*2012),Some researchers have used color indices to estimate herbaceous biomass (Bendig *et al.,*2014; Lussem *et al.,* 2018; Possoch *et al.,* 2016). A similar study by other researchers used an unmanned aerial vehicle (UAV) and a ground-based digital camera, combined with above-ground herbaceous biomass measurements, to estimate herbaceous biomass with mean estimation errors of around 150 g/m² for fresh mass (relative error of 20%) and 60 g/m² for dry mass (error of around 25%) and a coefficient of determination R^2

equal to 0.60(Taugourdeau *et al.,* 2022). In our study, some errors in predicting herbaceous biomass could also be attributed to manual measurements of herbaceous vegetation (destructive sampling) and to the simulation of GPS points in the quadrats. The use of ground markers could reduce these errors and enable more accurate location of the 1 m² quadrats (Bossoukpe *et al.,* 2021).The results of the drone assessment of woody trees enabled us to distinguish variations of between 74% and 89% in individual measurements of total height obtained from one site to another compared with field measurements. These results are in line with those obtained by other researchers in Senegal (Bossoukpe, 2021 ; Sarron, 2019),where 85% of the heights obtained by drone imagery were equal to those measured in the field. Similar results were also observed by researchers in Burkina Faso (Konaté*et al.,* 2022),where 91% of the height in the field corresponded to that obtained from drone images. However, in our study, the highest correlation (R^2 = 0.89) was observed at the Oroubeidou site in Benin, due to the relative size of the species inventoried. In fact, the position of certain trees may overestimate the height estimated by photogrammetry, as the drone cannot see beneath the trees. In addition, the large sample size may also lead to measurement errors in the field. Our results are similar to those obtained by researchers in Spain(Zarco-Tejada *et al.,* 2014)who used a fixed-wing drone to estimate tree heights over a 158-hectare forest area. The method used was automatic 3D reconstruction, generating an orthomosaic and digital surface models of the study area. Photogrammetric crown area measurements were also 80% correlated with field measurements. Our results are similar to those obtained by other researchers (Bossoukpe et *al*., 2021; Konaté *et al.,*2022; Lisein, 2016; Tu *et al*.,2019), who used photogrammetry to estimate the surface area of a tree's crown. The results of woody biomass prediction, based on dendrometric parameters and drone measurements (height, NDVI), showed that woody biomass was related to area and height variables, and not to NDVI vegetation indices. The explanatory variables (R^2) varied from 0.58 to 0.69 between the height estimated by the drone and woody biomass. These results confirm those obtained by other researchers (Panday *et al.,* 2020) and (Bossoukpe et *al.,* 2021)who found that 41% of the variability in woody phytomass was not explained by any drone output. However, the inaccuracy of our assessment could be due to our method of calculating woody phytomass. We used allometric equations based on trunk diameter and average crown area. In addition, we used pantropical equations for certain species for which specific equations were not available(Brown, 1997). Another source of inaccuracy could be the flight altitude, as we flew at 90 meters. Differentiating the flight altitude could enable us to obtain more precise heights than those obtained at 90 meters, and improve the accuracy of the woody biomass estimate.

CONCLUSION

This study demonstrates the feasibility of using a low-cost multispectral drone to estimate herbaceous and woody biomass in the Sahelo-Sudanian and Sudanian zones. The results show that model parameters vary from site to site, as evidenced by the R^2 values. R^2 regression coefficients ranged from 0.59 to 0.86 for herbaceous biomass, and from 0.58 to 0.69 for woody biomass. It is important to note that despite these variations, the correlations remain significant ($P < 0.0001$) for all sites. Furthermore, the analyses reveal that the highest coefficient of determination is observed in the Sudanian zone, for both herbaceous and woody biomass. Root-mean-square errors (RMSE) and relative root-mean-square errors (RMSEr) also vary from site to site. They range from 0.013 kgMs/m² to 0.110 kgMs/m² (relative errors of around 19.86% to 26.84%) for herbaceous biomass, and from 0.53 kgMs/m² to 0.99 kgMs/m² (relative errors of around 14.16% to 39.55%) for woody biomass. The multispectral drone can be used as an intermediary tool between field measurements and the satellite images generally used for vegetation monitoring. Its use reduces the field sampling effort usually required to monitor vegetation in these pastoral areas. What's more, the multispectral drone makes it possible to bypass the disruption caused by clouds on satellite images during certain periods of the year.

Acknowledgements

We would like to express our sincere thanks to the managers of Component 1 of the Service Regional information sur le Pastoralism (SIRP) for their funding under the PREDIP program, supported by the European Union. We would also like to thank the administrative authorities of the Centre Regional AGRHYMET (CRA) and the Direction de Formation et de la Recherche (DFR) of the CRA for their support.

REFERENCES

Adamou, S., Amani, A., Mahamadou, H. M., & Yaye, A. D. (2020). Modèle allométrique d'estimation du carbone aérien séquestré par Balanites aegyptiaca (L.) Del dans la partie Sud-Ouest du Niger. *Afrique Science*, *16*(6), 188-203.

Anifantis, A. S., Camposeo, S., Vivaldi, G. A., Santoro, F., & Pascuzzi, S. (2019). Comparison of UAV photogrammetry and 3D modeling techniques with other currently used methods for estimation of the tree row volume of a super-high-density olive orchard. *Agriculture*, *9*(11), 233.

Barrachina, M., Cristóbal, J., & Tulla, A. F. (2015). Estimating above-ground biomass on mountain meadows and pastures through remote sensing. *International Journal of Applied Earth Observation and Geoinformation*, *38*, 184-192.

Bendig, J., Bolten, A., Bennertz, S., Broscheit, J., Eichfuss, S., & Bareth, G. (2014). Estimating biomass of barley using crop surface models (CSMs) derived from UAV-based RGB imaging. *Remote sensing*, *6*(11), 10395-10412.

Bossoukpe, F. O. M. (2021). *Etude de la végétation de savanes sahéliennes par photogrammétrie à partir d'appareil photographique compact et de drones low-cost, p85*.

Bossoukpe, M., Ndiaye, O., Diatta, O., Diatta, S., Audebert, A., Couteron, P., Leroux, L., Diouf, A. A., Dendoncker, M., & Faye, E. (2021). Unmanned aerial vehicle for the assessment of woody and herbaceous phytomass in Sahelian savanna. *Revue d'Elevage et de Médecine Vétérinaire des Pays Tropicaux*, *74*(4), 199-205.

Bourgoin, C., Betbeder, J., Couteron, P., Blanc, L., Dessard, H., Oszwald, J., Le Roux, R., Cornu, G., Reymondin, L., Mazzei, L., Sist, P., Läderach, P., & Gond, V. (2020). UAV-based canopy textures assess changes in forest structure from long-term degradation. *Ecological Indicators*, *115*, 106386. https://doi.org/10.1016/j.ecolind.2020.106386

Brown, S. (1997). *Estimating biomass and biomass change of tropical forests: A primer* (Vol. 134). Food & Agriculture Org.

Candiago, S., Remondino, F., De Giglio, M., Dubbini, M., & Gattelli, M. (2015). Evaluating multispectral images and vegetation indices for precision farming applications from UAV images. *Remote sensing*, *7*(4), 4026-4047.

Carlos A. Devia, Juan P. Rojas, E. Petro, Carol Martinez, Ivan F. Mondragon, D. Patino, M. C. Rebolledo & J. Colora-do. (2019). Estimation de la biomasse à haut débit dans les cultures de riz à l'aide de l'imagerie multispectrale UAV. *Journal des systèmes intelligents et robotiques*, *96*, 573-589.

CEDEAO, C. (2008). Elevage et marché régional au Sahel et en Afrique de l'Ouest: Potentialités et défis. *Transformation du monde rural et développement durable en Afrique de l'Ouest, Paris Cedex*, *16*, 182.

CILSS /RPCA (2010). *L'élevage au Sahel et en Afrique de l'Ouest. 26ème réunion annuelle du Réseau de Prévention des Crises Alimentaires (RPCA), 14-16 décembre 2010, Accra, Ghana—Recherche Google*.

Cunliffe, A. M., Brazier, R. E., & Anderson, K. (2016). Ultra-fine grain landscape-scale quantification of dryland vegetation structure with drone-acquired structure-from-motion photogrammetry. *Remote Sensing of Environment*, *183*, 129-143.

Daget, P., & Poissonet, J. (1971). *Une méthode d'analyse phytologique des prairies : Critères d'application*.

Diouf, A. A., Brandt, M., Verger, A., El Jarroudi, M., Djaby, B., Fensholt, R., Ndione, J. A., & Tychon, B. (2015). Fodder biomass

monitoring in Sahelian rangelands using phenological metrics from FAPAR time series. *Remote Sensing*, *7*(7), 9122-9148.

DRE. (2022). *Rapport Provisoire de la Situation Pastorale Direction Régionale de l'Elevage de Dosso 24 p.*

FAO Stat, faostat.fao.org/site/613/ Desktop Default. Aspx? PageID=613#ancor, (consulté le 03/02/2023).(2015).

Fernández-Guisuraga, J. M., Sanz-Ablanedo, E., Suárez-Seoane, S., & Calvo, L. (2018). Using unmanned aerial vehicles in postfire vegetation survey campaigns through large and heterogeneous areas: Opportunities and challenges. *sensors*, *18*(2), 586.

Gao, T., Xu, B., Yang, X., Jin, Y., Ma, H., Li, J., & Yu, H. (2013). Using MODIS time series data to estimate aboveground biomass and its spatio-temporal variation in Inner Mongolia's grassland between 2001 and 2011. *International Journal of Remote Sensing*, *34*(21), 7796-7810.

Garba, I., Djaby, B., Salifou, I., Boureima, A., Touré, I., & Tychon, B. (2015). ÉvaluatIon des RessouRces pastoRales au sahel nIgéRIen à l'aIde des donnéés ndvI Issues de spot-vegetatIon et modIs. *Photo interprétation European Journal of Applied Remote Sensing*, *1*(1), 13-26.

Gleason, C. J., & Im, J. (2012). Forest biomass estimation from airborne LiDAR data using machine learning approaches. *Remote Sensing of Environment*, *125*, 80-91.

Henry, M., Picard, N., Trotta, C., Manlay, R., Valentini, R., Bernoux, M., & Saint-André, L. (2011). Estimating tree biomass of sub-Saharan African forests: A review of available allometric equations. *Silva Fennica*, *45*(3), 477-569.

Hiernaux, P., Diawara, M. O., Kergoat, L., & Mougin, É. (2015). La contrainte fourragère des élevages pastoraux et agro-pastoraux du Sahel. *Book : Les sociétés rurales face aux changements climatiques et environnementaux en Afrique de l'Ouest. Editors: IRD https://www.researchgate. net/publication/303372607_*.

Hountondji, Y.-C. H. (2008). Dynamique environnementale en zones sahélienne et soudanienne de l'Afrique de l'Ouest : Analyse des modifications et évaluation de la dégradation du couvert végétal. *Belgique : Université de Liège*.

Khun, K. (2021). *Contribution de l'imagerie dronique pour la caractérisation des paramètres biophysiques des cultures agricoles*.

Koala, J. (2016). *Influence de perturbation anthropique sur le stock de carbone dans les écosystèmes de savane en zone soudanienne du Burkina Faso* [PhD Thesis]. Thèse de doctorat Unique, Institut du Developpement Rural, Université Nazi Boni.

Konaté, I., Dayanba, S. D., Koala, J., Tondé, N., Damoue, A. K., Sawadogo, L., & Hien, M. (2022). Prédiction des paramètres dendrométriques à l'aide des prises de vue de drone en zone soudanienne: Perspectives pour une évaluation rapide des stocks de carbone forestier. *Journal of Applied Biosciences*, *177*, 18514-18536.

Lisein, J. (2016). *Application des techniques de photogrammétrie par drone à la caractérisation des ressources forestières*.

Liu, H., Dahlgren, R. A., Larsen, R. E., Devine, S. M., Roche, L. M., O'Geen, A. T., Wong, A. J., Covello, S., & Jin, Y. (2019). Estimating rangeland forage production using remote sensing data from a small unmanned aerial system (sUAS) and planetscope satellite. *Remote Sensing*, *11*(5), 595.

Lussem, U., Bolten, A., Gnyp, M., Jasper, J., & Bareth, G. (2018). Evaluation of RGB-based vegetation indices from UAV imagery to estimate forage yield in grassland. *The International Archives of the Photogrammetry, Remote Sensing and Spatial Information Sciences*, *42*(3), 1215.

Lussem, U., Bolten, A., Menne, J., Gnyp, M. L., Schellberg, J., & Bareth, G. (2019). Estimating biomass in temperate grassland with high resolution canopy surface models from UAV-based RGB images and vegetation indices. *Journal of Applied Remote Sensing*, *13*(3), 034525-034525.

Mahamane.A, Mahamane. S, Karim S, Bakasso.Y, Boubé .M, Issoufou. W, Abdoulaye. D, Inoussa M. M, Abassa. I, Arzika. T, Idrissa. S.M et Sandrine. J. (2004). *Variabilité climatique au Niger : Impacts potentiels sur la distribution de la végétation.*

Mbow, C., Verstraete, M. M., Sambou, B., Diaw, A. T., & Neufeldt, H. (2014). Allometric models for aboveground biomass in dry savana trees of the Sudan and Sudan-Guinean ecosystems of Southern Senegal. *Journal of Forest Research*, *19*(3), 340-347.

Météo Bénin. (2018). *Données climatiques des stations météorologiques de Banikoara, Kérou, Kandi, Karimama, Malanville, Natitingou. Agence Nationale de Météorologie, Cotonou.*

Ndamiyehe Ncutirakiza, J.-B., Lejeune, P., Gourlet-Fleury, S., Fayolle, A., Ndjele Mianda-Bungi, L., & Ligot, G. (2020). Quantifier les dimensions des houppiers à l'aide d'images aériennes à haute résolution pour estimer l'accroissement diamétrique des arbres dans les forêts d'Afrique centrale. *Bois et Forêts des Tropiques*, *343*.

Ngabinzeke, J. S., Linchant, J., Quevauvillers, S., Muhongya, J.-M. K., Lejeune, P., & Vermeulen, C. (2016). Cartographie de la dynamique de terroirs villageois à l'aide d'un drone dans les aires protégées de la République démocratique du Congo. *BOIS & FORETS DES TROPIQUES*, *330*, 69-83.

Nungi-Pambu, M. (2022). *Utilisation des drones comme étape intermédiaire pour la cartographie de la végétation à l'échelle nationale : Exemple du Sénégal*.

Panday, U. S., Shrestha, N., Maharjan, S., Pratihast, A. K., Shahnawaz, Shrestha, K. L., & Aryal, J. (2020). Correlating the plant height of wheat with above-ground biomass and crop yield using drone imagery and crop surface model, a case study from Nepal. *Drones*, *4*(3), 28.

Peciña, M. V., Bergamo, T. F., Ward, R., Joyce, C., & Sepp, K. (2021). A novel UAV-based approach for biomass prediction and grassland structure assessment in coastal meadows. *Ecological Indicators*, *122*, 107227.

Pham, T. D., Yoshino, K., & Bui, D. T. (2017). Biomass estimation of Sonneratia caseolaris (l.) Engler at a coastal area of Hai Phong city (Vietnam) using ALOS-2 PALSAR imagery and GIS-based multi-layer perceptron neural networks. *GIScience & Remote Sensing*, *54*(3), 329-353.

Possoch, M., Bieker, S., Hoffmeister, D., Bolten, A., Schellberg, J., & Bareth, G. (2016). Multi-temporal crop surface models combined with the RGB vegetation index from UAV-based images for forage monitoring in grassland. *The International Archives of Photogrammetry, Remote Sensing and Spatial Information Sciences*, *41*, 991.

Puliti, S., Ørka, H. O., Gobakken, T., & Næsset, E. (2015). Inventory of small forest areas using an unmanned aerial system. *Remote Sensing*, *7*(8), 9632-9654.

Read, J. M., Clark, D. B., Venticinque, E. M., & Moreira, M. P. (2003). Application of merged 1-m and 4-m resolution satellite data to research and management in tropical forests. *Journal of applied ecology*, *40*(3), 592-600.

Reinermann, S., Asam, S., & Kuenzer, C. (2020). Remote sensing of grassland production and management—A review. *Remote Sensing*, *12*(12), 1949.

Roupsard, O., Audebert, A., Ndour, A. P., Clermont-Dauphin, C., Agbohessou, Y., Sanou, J., Koala, J., Faye, E., Sambakhe, D., & Jourdan, C. (2020). How far does the tree affect the crop in agroforestry? New spatial analysis methods in a Faidherbia parkland. *Agriculture, Ecosystems & Environment*, *296*, 106928.

Ruzgienė, B., Berteška, T., Gečyte, S., Jakubauskienė, E., & Aksamitauskas, V. Č. (2015). The surface modelling based on UAV Photogrammetry and qualitative estimation. *Measurement*, *73*, 619-627.

Sarron, J. (2019). *Estimation spatialisée des rendements d'une culture pérenne en Afrique de l'Ouest : Le cas du manguier au Sénégal* [PhD Thesis]. Montpellier SupAgro.

Sawadogo, L., Savadogo, P., Tiveau, D., Dayamba, S. D., Zida, D., Nouvellet, Y., Oden, P. C., & Guinko, S. (2010). Allometric prediction of above-ground biomass of eleven woody tree species in the Sudanian savanna-woodland of West Africa. *Journal of Forestry Research*, *21*, 475-481.

Surault, F., Roy, E., Escobar-Gutiérrez, A. J., & Barre, P. (2018). Le drone, un nouvel outil au service de la sélection pour estimer la hauteur des plantes fourragères. *Fourrages*, *236*, 281-288.

Surový, P., Almeida Ribeiro, N., & Panagiotidis, D. (2018). Estimation of positions and heights from UAV-sensed imagery in

tree plantations in agrosilvopastoral systems. *International Journal of Remote Sensing*, *39*(14), 4786-4800.

Taugourdeau, S., Diedhiou, A., Fassinou, C., Bossoukpe, M., Diatta, O., N'goran, A., Auderbert, A., Ndiaye, O., Diouf, A. A., & Tagesson, T. (2022). Estimating herbaceous aboveground biomass in Sahelian rangelands using Structure from Motion data collected on the ground and by UAV. *Ecology and Evolution*, *12*(5), e8867.

Taule, M. D. P., Morissette, S., Ménard, P., & Jean, K. (2012). *L'imagerie multispectrale comme outil d'analyse et de diagnostic pour la productivité des sols en agriculture de précision*.

Tu, Y.-H., Johansen, K., Phinn, S., & Robson, A. (2019). Measuring canopy structure and condition using multi-spectral UAS imagery in a horticultural environment. *Remote Sensing*, *11*(3), 269.

Wijesingha, J., Astor, T., Schulze-Brüninghoff, D., Wengert, M., & Wachendorf, M. (2020). Predicting forage quality of grasslands using UAV-borne imaging spectroscopy. *Remote Sensing*, *12*(1), 126.

Zahawi, R. A., Dandois, J. P., Holl, K. D., Nadwodny, D., Reid, J. L., & Ellis, E. C. (2015). Using lightweight unmanned aerial vehicles to monitor tropical forest recovery. *Biological Conservation*, *186*, 287-295.

Zarco-Tejada, P. J., Diaz-Varela, R., Angileri, V., & Loudjani, P. (2014). Tree height quantification using very high-resolution imagery acquired from an unmanned aerial vehicle (UAV) and automatic 3D photo-reconstruction methods. *European journal of agronomy*, *55*, 89-99.

****